Supplementary Materials: Enantioselective Transamination in Continuous Flow Mode with Transaminase Immobilized in a Macrocellular Silica Monolith

Ludivine van den Biggelaar, Patrice Soumillion and Damien P. Debecker

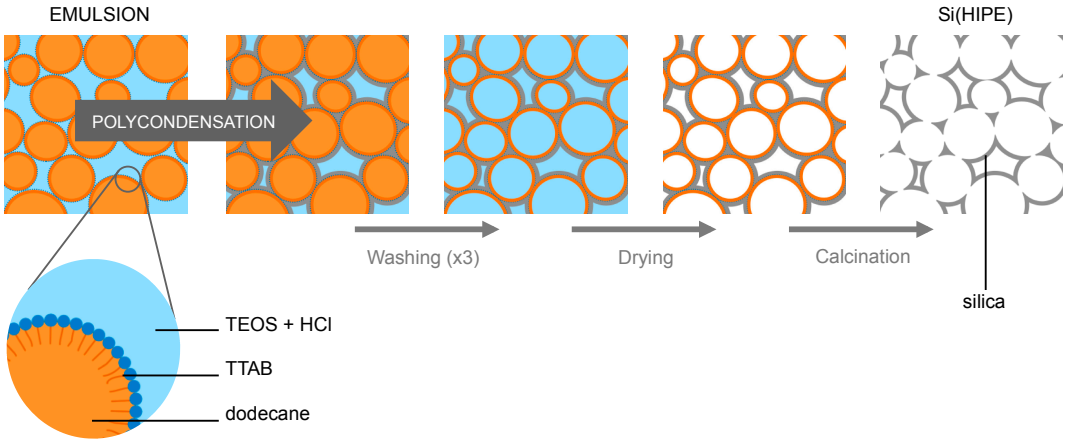

Figure S1. Si(HIPE) monolith synthesis. An amount of 6 g of a concentrated hydrochloric acid solution (37% wt) was introduced in 16 g of a TTAB aqueous solution (35% wt). Then, 5 g of TEOS was added. The aqueous phase was stirred until a monophasic hydrophilic medium was obtained. To form an emulsion, 35 g dodecane was then added dropwise in a mortar while stirring. Emulsion was cast into a polypropylene 10 mL flask, and allowed to condense for 1 week at room temperature. Resulting material was washed three times with 50 mL of a THF/acetone mixture (1:1 *v*/*v*) (each washing lasted 24 h) and then gently dried in air for 3 days before being calcined at 650 °C for 6 h (heating rate of 2 °C/min with a first plateau at 180 °C for 6 h). Porous monoliths were stored in a desiccator at room temperature.

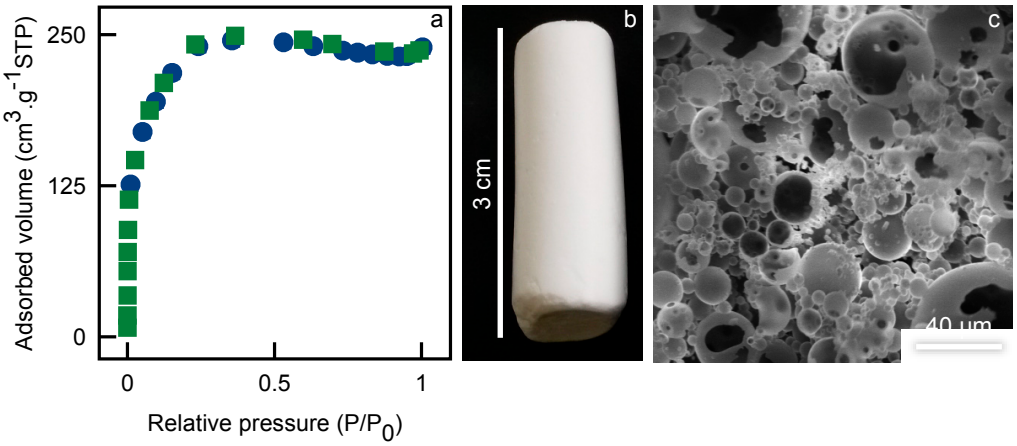

Figure S2. (**a**) Nitrogen (□) adsorption and (●) desorption isotherms. Specific surface area reaches 820 $m^2.g^{-1}$, mainly explained by microporosity due to silica lattice molecular structure; (**b**) Cylindrical Si(HIPE) monolith of ~3.5 cm in height and ~0.9 cm in diameter. Each monolith weighs approximately 0.15 g. Monoliths density is 0.0628 g/cm^3 and porosity reaches ~95% (if bulk density is assumed to be 1.56 g·cm^{-3}) [30]; (**c**) Si(HIPE) consists of empty interconnected spherical silica shells whose shape is a reminiscence of the dodecane droplets in the oil-in-water emulsion. Polycondensation of TEOS into silica starts from the organic/aqueous interface towards the rest of aqueous phase [30]. The diameter of the macrocellular shells is highly variable (from ~1 µm to 300 µm). Monoliths macroporous structure observed in SEM can be quantitatively confirmed by Hg-porosimetry, as already reported [30].

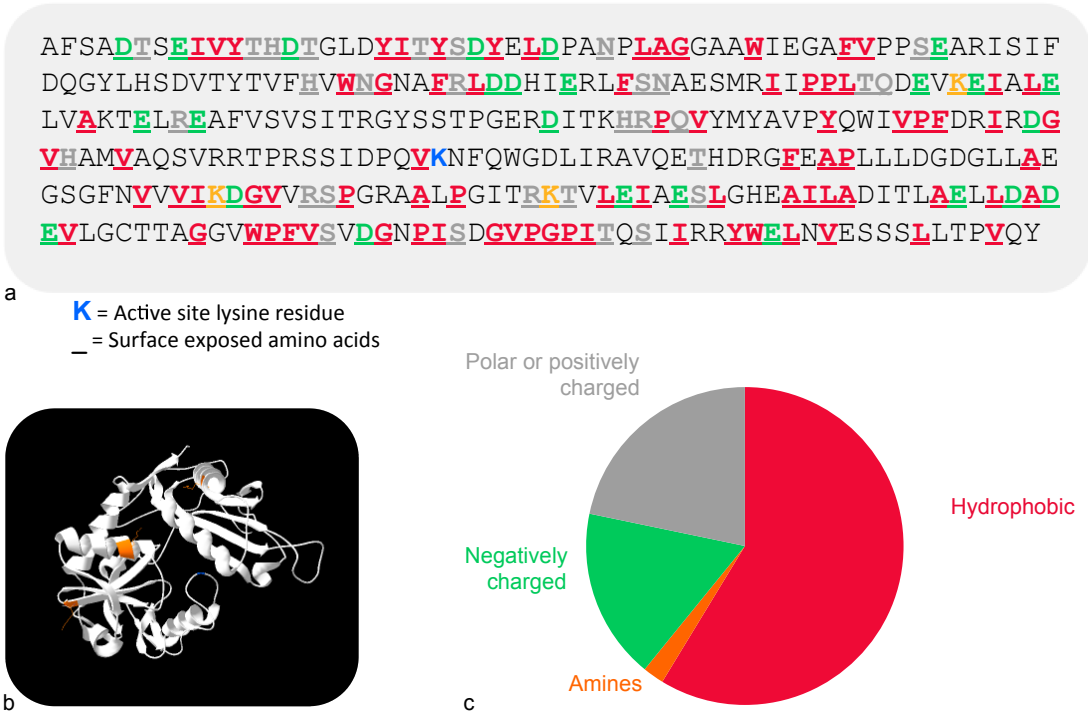

Figure S3. (**a**) ATA-117 protein sequence. Underlined residues are located at the external surface of the enzyme. Colors refer to chemical types; (**b**) ATA-117 monomer unit. The 3D structure of ATA-117 has been published recently [42] (structure entry on PDBe: 3wwh). The PISA Tool (Proteins, Interfaces, Structures and Assemblies) [43] provides the relative position of each amino acid: (i) solvent-accessible residues (external surface), (ii) interfacing residues, or (iii) inaccessible residues (located in the enzyme structure); (**c**) Ratios of chemical functions at the external surface: more than half of the amino acids located at the surface are hydrophobic residues. A large part of the residues are polar or charged.

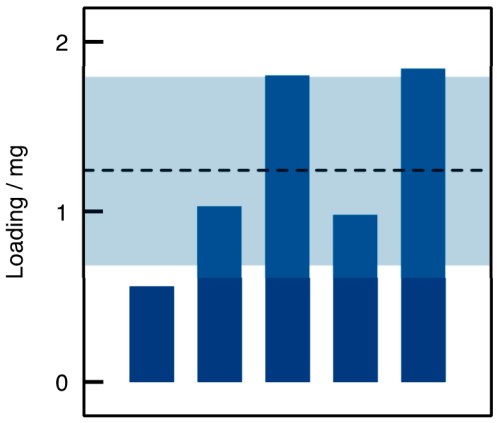

Figure S4. Measurement of the enzyme loading in TA-A50 (five experiments). Dotted line represents the mean value (1.2 mg); shaded area represents the relative standard deviation (RSD is 45%).

Discussion. Determination of enzyme loading in the monoliths was delicate. For enzyme immobilization, 50 mL of a glutaraldehyde buffered solution is flowed through the flow reactor. Then, 50 mL of ATA-117 solution with an initial concentration of 0.2 mg/mL (C_0) is flowed. An amount of 50 mL of outflow is collected and the enzyme concentration is measured (C_1). Finally, the reactor is washed with 50 mL of buffer solution (no enzyme) and 50 mL is collected at the outflows (C_2). The loading (L; in mg) is determined by mass balance: $L = 50\ \text{mL} \times (C_0 - C_1 - C_2)$. However, obtained loading values were often low, sometimes negative (see discussion in Figure S5), and suffered from high variability. We ensured that there was neither contamination nor interference involved in the loading

determination. Concentration measurement using the Bradford method was very precise. Temperature sensibility, reactants instability, and stirring method have also been studied but showed no influence on the measurement. Only the catalysts functionalized with high amount of APTES provided relevant loading measurements, yet repeatability was poor, as shown above. For the catalysts with low APTES concentration or no APTES at all, we can only safely say that the loading is lower than 0.5 mg.

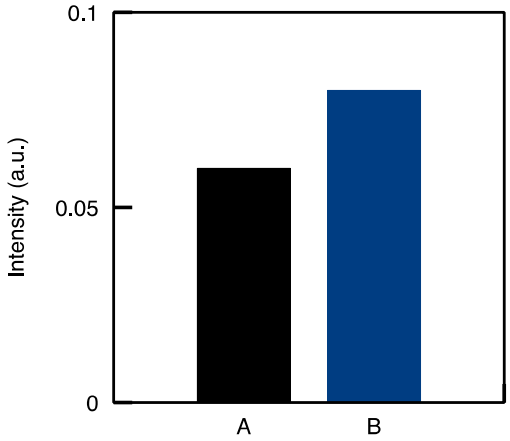

Figure S5. Dynamic light scattering (DLS) signal intensity around 3 nm for ATA-117 solution (**A**) before and (**B**) after passing through the flow set-up. Relative standard deviation is 15%.

Discussion. By the Bradford method, we observed that enzymatic solution concentration sometimes increased by passing through the flow set-up, even without monolith. This suggests that the initial enzyme solution used to load the monolith may contain enzymatic aggregates that are broken only under flow constraints. Those aggregates are a source of variability (C_0 is underestimated in the Bradford measurement). DLS tends to confirm the aggregates hypothesis. Indeed, for enzyme solution outflows, a higher scattering intensity was observed around 3 nm (i.e., close to the size of single enzyme molecules). This may indicate a larger proportion of free enzyme. The presence of aggregates in the initial solution causes high variability in the loading measurement. Therefore, we are limited to a rough estimation of the loading measurement.

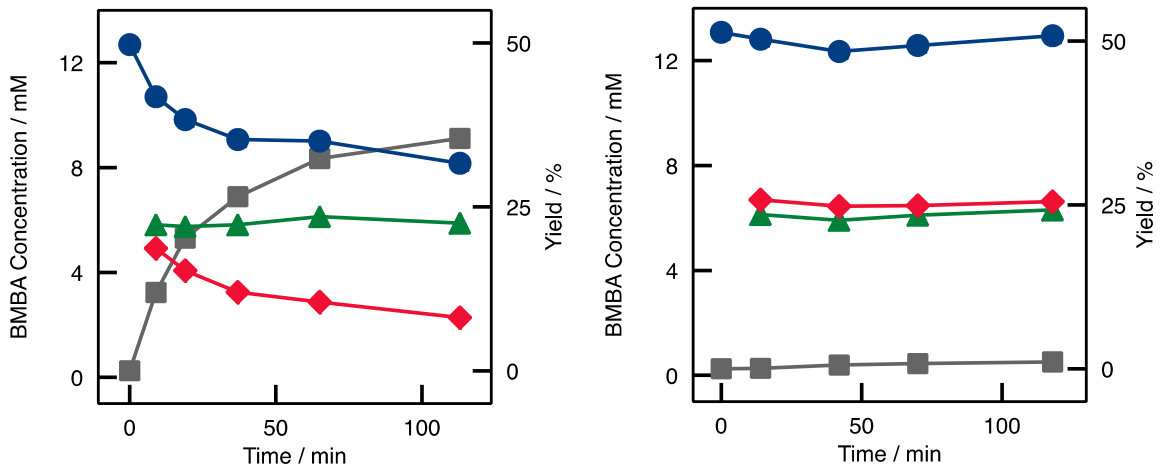

Figure S6. Kinetic resolution of racemic bromo-α-methylbenzylamine (rac-BMBA) into 4′-bromoacetophenone (BAP) in batch mode. Total BMBA concentration is assessed by GC, and enantiomeric excess is assessed by chiral-HPLC. (■) Yield is obtained by measuring the BAP concentration in GC. (**a**) Batch transamination with ATA-117 (0.2 g/L): (●) total BMBA concentration decreases with time. Only *R*-BMBA (◆) is converted by ATA-117 while *S*-BMBA (▲) remains stable.

(**b**) Batch transamination without ATA-117: (●) BMBA (both *S* (◆) *S* and *R* (▲) enantiomers) is not converted significantly, confirming the very slow kinetics of the non-catalyzed reaction.

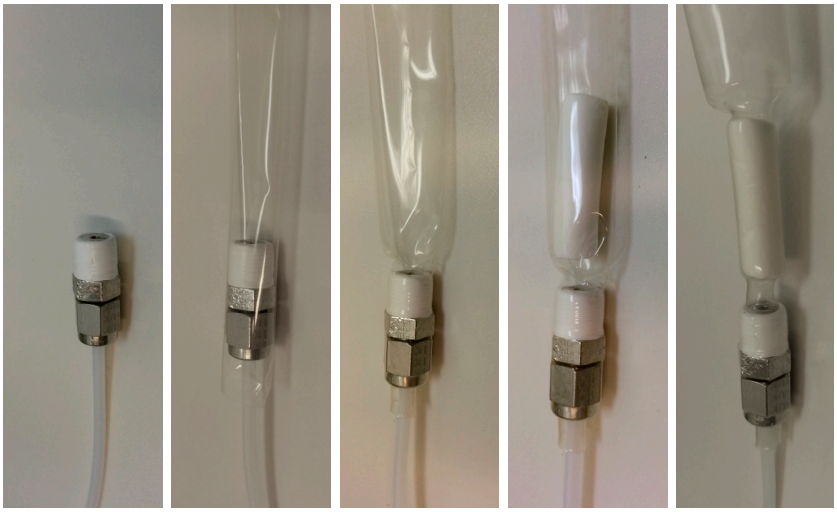

Figure S7. During the synthesis process, Si(HIPE) monoliths undergo an important macroscopic shrinkage attributed to the densification of the silica network. Consequently, it was impossible to predict the final diameter of the monoliths, and so, to build a suitable reactor for each batch of Si(HIPE). Therefore, a heat-shrinkable material was implemented to match the shapes of the monolith. This plastic material shrinks when heated, without damaging the monolith. A polytetrafluoroethylene heat-shrinkable membrane—inert towards flow components—was implemented. Syringe-pumps connected to PTFE tubes and syringes were chosen as inert pumping devices.

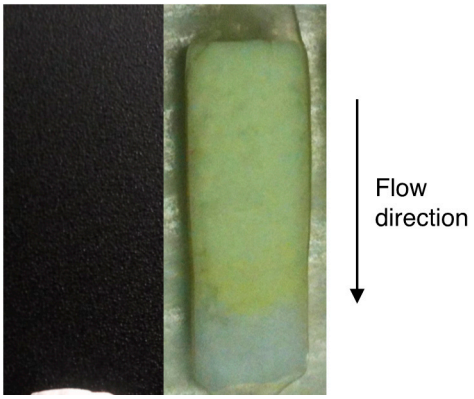

Figure S8. Prior to flow biocatalysis experiments, the buffer (which contains PLP, a yellow compound) was injected into a Si(HIPE) monolith, itself placed in the continuous flow set-up. The flow was stopped before the yellow coloration reached the end of the monolith. The monolith was then recovered and cut lengthwise in order to observe the flow profile. The boundary between the yellow zone (filled with buffer) and the white zone (not yet reached by the buffer) is straight. Also, to the eye, the yellow zone is uniform in colour intensity. This indicates that the liquid follows an ideal plug flow regime into Si(HIPE). Therefore, it is assumed that product concentration into the reactor depends only on the relative position on the axis parallel to the flow (rather than on the radial position).

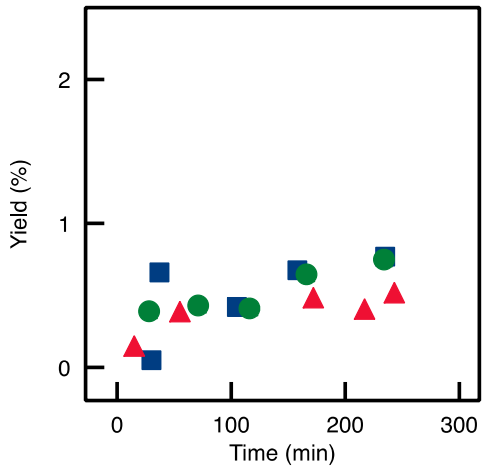

Figure S9. Kinetic resolution of racemic bromo-α-methylbenzylamine (rac-BMBA) into 4′-bromoacetophenone (BAP) in flow mode using (■) Si(HIPE) or (▲) A50 monolith (no enzyme). Only a small conversion is observed (yield ~0.5%), corresponding to the slow non-enzymatic activity occurring in the stock solution under the sole effect of PLP, as observed also in batch mode (●) in the same conditions.

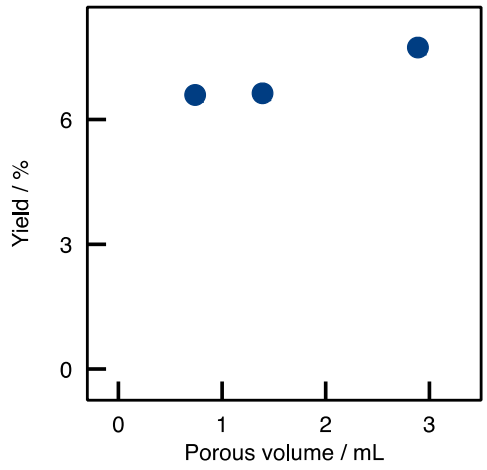

Figure S10. Dependence of activity on flow rate. Contact time is maintained constant by adjusting the flow rate proportionally to the bed size. The yield was constant, suggesting that no diffusional limitation occurred for the flow rates chosen. To account for small variation in the monolith pore volume, data are plotted as a function of porous volume.

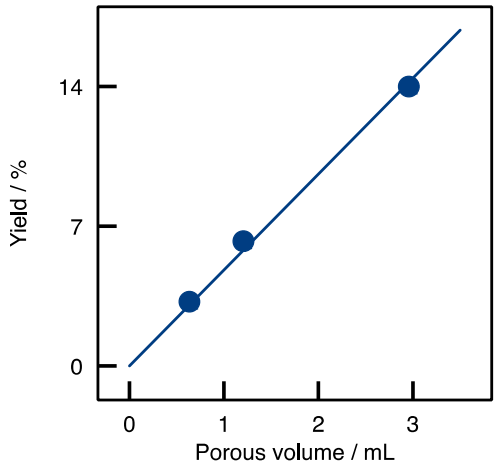

Figure S11. Dependence of activity on contact time, for TA-A50-GA. Flow rate was maintained constant but the size of the monolith was varied.